https://rbgeomorfologia.org.br/
ISSN 2236-5664

Revista Brasileira de Geomorfologia

v. 27, nº 1 (2026)

https://dx.doi.org/10.20502/rbg.v27i1.2694

Research Article

Characterization of surface materials and the relationship with topographic positions: case study in the Serra da Canastra, Brazil

Silvio Carlos Rodrigues [1], Thallita Isabela Silva Martins Nazar [2], Lukasz Pawlik [3], Fabiana Cristina dos Santos[4]

[1] Universidade Federal de Uberlândia, Instituto de Geografia, Geociências e Saúde Coletiva, Uberlândia, Brasil. silgel@ufu.br.
ORCID: https://orcid.org/0000-0002-5376-1773

[2] Universidade Federal de Catalão, Instituto de Geografia, Catalão, Brasil. thallitanazar@ufcat.edu.br.
ORCID: https://orcid.org/0000-0002-0257-1451

[3] University of Silesia in Katowice, Faculty of Natural Sciences, Katowice, Poland. lukpawlik@gmail.com,
ORCID: https://orcid.org/0000-0001-9271-3507

[4] Universidade Federal de Uberlândia, Instituto de Geografia, Geociências e Saúde Coletiva, Uberlândia, Brasil. fabianaqgufu@gmail.com
ORCID: http://orcid.org/0000-0001-6670-5212

Received: 16/04/2025; Accepted: 17/12/2025; Published: 04/02/2026

Abstract: Quartzite regions tend to present incipient and unconsolidated surface materials, even in areas with humid tropical climates. The degree of weathering of surface materials and its relationship to topography in these environments remains unknown. Therefore, the objective of this study is to analyze the relationship between topography and the mineralogy of the clay fraction of surface materials developed in quartzite bedrock. We selected three representative slopes along which transects were installed from the crest to the valley floor. Nine geocover samples were collected for analysis by X-ray diffraction. The results were analyzed using the Principal Component Analysis method. The results show a correlation between the identified materials, their position on the slope, the slope profile, and the presence of natural barriers. In the first transect, representing a quartzite ridge with extremely incipient weathering material, minerals indicative of highly weathered environments with poor drainage, such as kaolinite and illite, were found. In the second transect, representing broad interfluves with long slopes and low gradients, samples presented Fe and Al oxides and hydroxides, demonstrating the advanced degree of weathering in the area. The third transect, conducted in a secondary divide with a convex profile, collected a deeper sample containing goethite and siderite, indicating a poorly drained environment with water remaining in the system for a short time. Thus, it can be seen that, despite the predominantly quartzite basement, the shape of interfluves and slopes allows for differentiated development of the weathering mantle materials, strongly dependent on drainage dynamics and varying along the slope as a function of changes in longitudinal profiles.

Keywords: Quartzite slopes; Clay minerals; Surface materials.

1. Introduction

Geocovers, or surface materials, are records of geomorphological processes such as physical and chemical weathering that occurred and still form on lands and provide evidence on the landscape evolution and dynamics (CAMPY; MACAIRE, 1989; QUEIROZ NETO, 2001). Nazar and Rodrigues (2019a) conceived geocovers as the alteration materials covering the Earth's surface, including unconsolidated and consolidated materials such as

rocky outcrops and weathering-limited hillslopes. This definition encompasses the geomorphological studies in areas where the pedogenetic processes are incipient.

In quartzite areas of humid tropical environments, it is relevant to bring to light the role of weathering agents on such rocks, demonstrating the climate-rock-relief-biota relationship, in addition to leading to understanding of the area as a geomorphological system as an open system composed of forms, processes, and the relationship between the two.

Humid tropical regions are recognized for the intensity of the action of weathering processes and the formation of thick layers of soils that cover the slopes (VIDAL-TORRADO et al., 1999; EMBRAPA, 2018; PEREIRA et al., 2020). On the other hand, quartzite areas under such climate conditions tend to present incipient soils or without any evidence of weathering, with the exposure of rocks on more inclined slopes. However, a study gap can be observed in the literature in respect to the relationship between topography and geocovers in areas of quartzite relief.

Therefore, this study seeks to analyze the relationship between the topography and mineralogy of the clay fraction found in the geocovers developed on quartzite forming complex relief of the Serra da Canastra, on the surface of Chapadão do Diamante (ChD).

2. Methodology

The ChD is located in the municipality of São Roque de Minas, around 320 km from Belo Horizonte, the capital of the state of Minas Gerais, and approximately 300 km from Uberlândia, in the Triângulo Mineiro (Minas Triangle). Its delimitation is based on an altitude of 1,080 m, which is the maximum altitude limit from which the scarps that surround the area begin, making up a total area of 333 km2. Figure 1. According to Rodrigues et al. (2023a), the study area is located in the domain of the Serras and Mountains of Central Brazil, in the geomorphological unit known as Serra da Canastra.

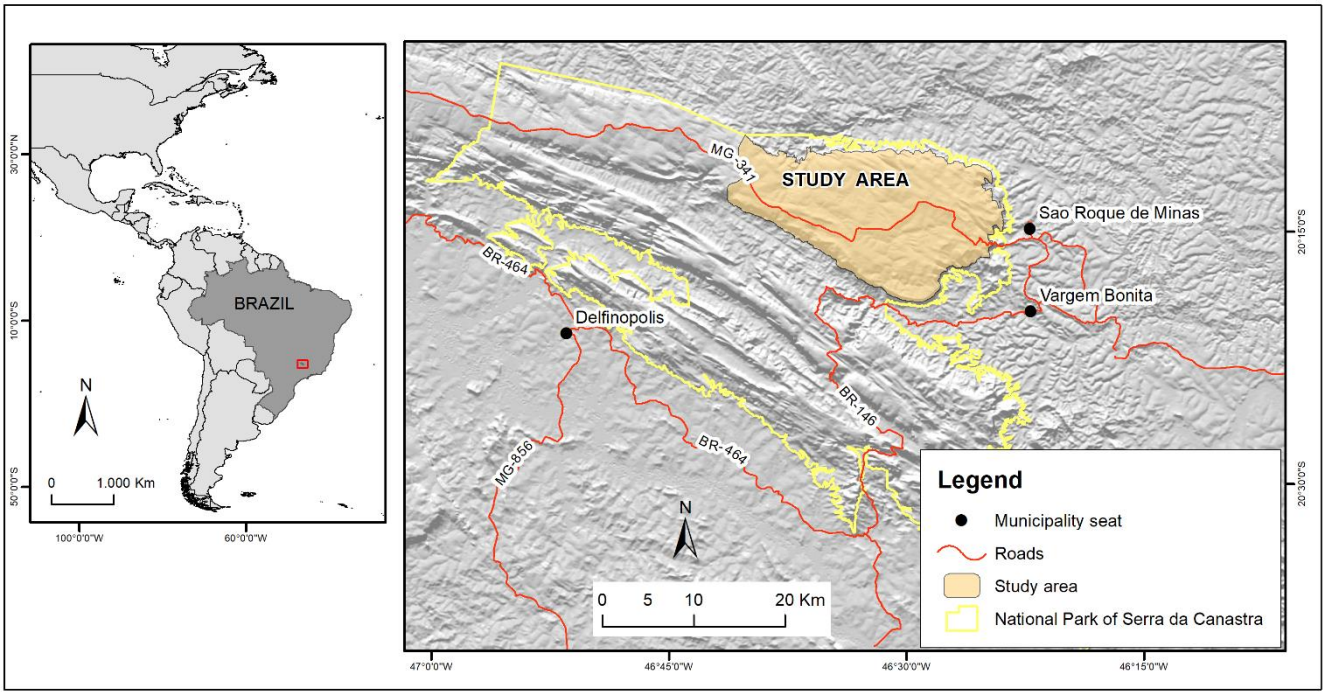

Figure 1. Relief of the study area in the context of Brazilian territory. Source: The authors.

The area is located in a region with a typical tropical seasonal climate, with two well-defined seasons: the wet season, characterized by a water surplus in the quarter from December to February; and the dry season, which occurs more pronounced between June and August, which are also the coldest months. Rainfall varies between 1,000 and 1,500 mm, and the average temperature ranges from 18°C in the coldest month to 22°C in the hottest

month (NOVAIS, 2011). It is worth highlighting the role of relief as an orographic factor, which differentiates temperatures and thermal sensations at the top of the Serra da Canastra, favoring and influencing the vegetation aspects of the ChD, given the altitudes that vary from 1,080 m to almost 1,500 m.

According to Valeriano et al. (2004), the geological structure of the study area comprises the geological framework of the Southern Brasília Belt, a NW-trending branch of the Neoproterozoic Orogenic System of the Tocantins Province. The Southern Brasília Belt originates from the interaction between the Paranapanema and São Francisco cratons and encompasses the mountainous relief belt of the Serra da Canastra. The lithologies that characterize this area are represented by the Canastra Group, subdivided into Formal Units and Indeterminate Canastra. The latter is formed by two lithostratigraphic units: the lower, consisting of a package of banded phyllites intercalated with quartzites (metarenite) that encompasses the edge of the mountain range; and the upper, composed of a package of pure to micaceous quartzites with rare intercalations of muscovite phyllite that constitute the central package of the mountain range where the research was conducted. being responsible for supporting the Serra da Canastra, where the ChD is located, as illustrated in Figure 2 (SIMÕES et al., 2015).

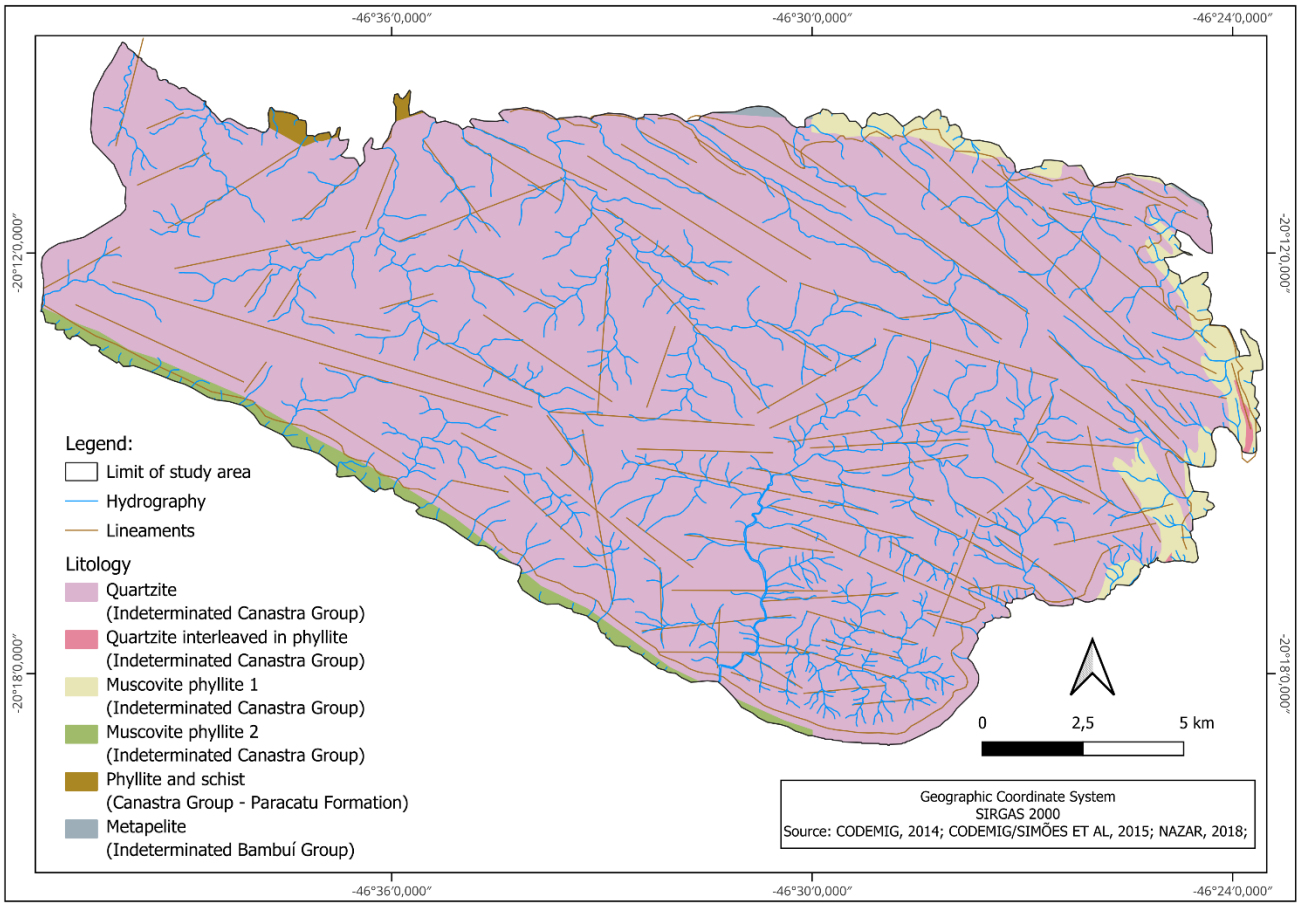

Figure 2. Geological map of the study area. Source: The authors.2024

Nazar and Rodrigues (2019) present a study on the distribution of geocovers in the Serra da Canastra. In this study, they observe that more than half of the ChD covers are composed of sandy and gravelly materials with rocky outcrops, indicating the prominent role of the lithological type present there, quartzite. In addition, about 20% of the area was recognized with the presence of ferruginous materials, with even significant occurrences of lateritic concretions. This study demonstrates that there is a relationship between the distribution of geocovers partially associated with the relief patterns identified in the ChD study.

In this way, Nazar and Rodrigues (2019a) demonstrate that Flattened Relief unit associated with interfluves, it is noted that more than 70% of the sandy-clayey-ferruginous geocovers with ferruginous concretions occupy these areas, while approximately 40% of the murundun fields or ferruginous bioturbation materials are found in

these locations. Thirdly, there are sandy gravel materials with ferruginous concretions, with approximately 30% of their total distributed on flat tops.

For the Gently Dissected Relief class, the geocovers with the largest distributed areas are the undifferentiated murundun fields (>50%), the gravel-sandy materials with ferruginous concretions (~45%), and the murundun fields (~45%). undifferentiated sandy-clayey materials (~45%), ferruginous murundun fields (40%), and finally, gravelly-sandy materials with an organic layer (~35%). In the dissected relief unit on undulating hills, the materials are distributed more evenly, with emphasis on organic geocovers, undifferentiated sandy-clayey materials, and undifferentiated gravelly-sandy materials, both with approximately 30% of their areas devoted to this type of relief. Regarding the strongly dissected relief pattern, organic materials and undifferentiated gravelly-sandy materials stand out, accounting for approximately 20% of their areas.

The geocovers of rocky outcrops and gravelly-sandy materials with blocky chaos have the majority of their areas, approximately 40% and 30%, respectively, allocated to the relief pattern of elongated quartzite ridges. Undifferentiated colluvial materials, in turn, occur mostly (>60%), associated with the relief pattern of structural escarpments. The latter also receives approximately 20% of the total quartzite outcrops. These last two relief classes tend to have less variation in the types of geocovers found in the ChD, given their structure in quartzite rocks, which are quite resistant to weathering processes.

During the fieldwork stage of the study we collected control points (GPS) and a photographic record, with imaging being carried out through unmanned aerial vehicle – UAV. This stage contributed to the recognition, observation and interpretation of the landscape, relief forms, geomorphological phenomena, and surface materials, as well as to soil material collection at certain points of the sampling areas.

Figure 3 shows the selection of three sampling areas for the collection of surface materials, based on transects along the interfluve-valley floor axis, on three main types of slope. The choice of transects is according to the different classes of relief mapped by Nazar and Rodrigues (2019b). This choice aimed to establish the relationship between the geocovers and the topography, according to the main landscape patterns initially observed:

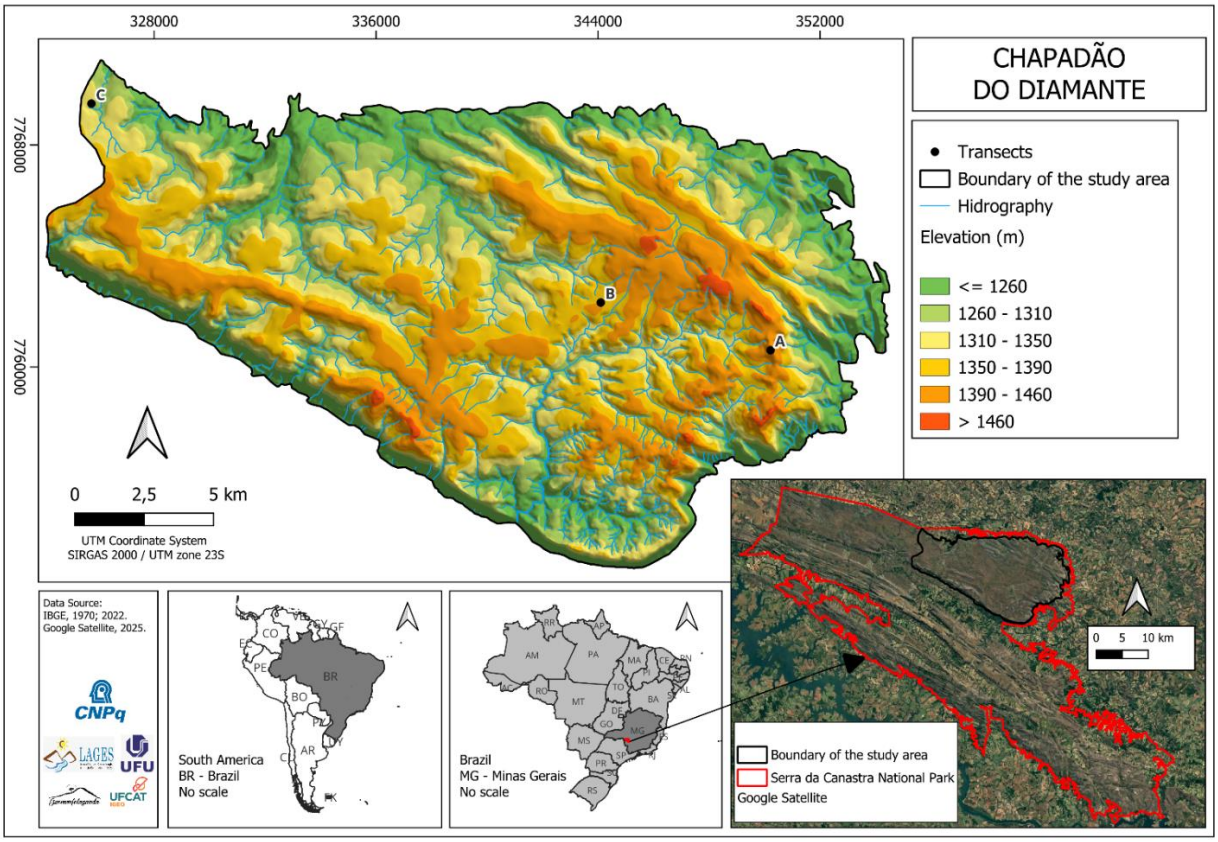

Figure 3. Location of samples area and transects. Source: The authors (2025)

Transect A is 510 meters long, starting at the top of the ridge and extending to a structural level made of quartzite. It is associated with a steep quartzite ridge relief with quartzite outcrops of the blocky chaos type. Thus, the geocovers were mapped as Sandy Gravel Materials with Blocky Chaos (Nazar and Rodrigues, 2019b), representing superficial materials associated with the decomposition of pure quartzites to micaceous materials. The deposits occur in an intrablock situation, at shallow depth, with a predominant presence of gravel and sand. (Figure 4)

Transect B is 580 meters long and was constructed in gently undulating terrain, comprising a section between the flat interfluve, a small flat plateau, with an initially straight slope becoming concave, and rare rocky outcrops. The geocovers vary in thickness, with a predominance of the sandy-clayey-ferruginous type with ferruginous concretions. Termite mounds also occur in various topographic positions, preferably in straight-concave sections, and fine and coarse, dark gray materials can be observed at the bottom of the valleys, composing the organic geocovers, associated with the slow decomposition of organic matter. Figure x.

Transect C follows a flat, gently undulating relief pattern with a convex-concave profile and is only 200 meters long. It begins in a secondary interfluve, where thick materials of the Sand-Clay-Ferruginous geocovers with Ferruginous Concretions occur. There are no rock outcrops, and the alteration layers exceed 1 meter in thickness. Mounded fields and organic material are also present in the river valley. The vegetation consists of grasslands, shrublands, and cerrado stricto sensu (Savannah) (Figure 3 and 4).

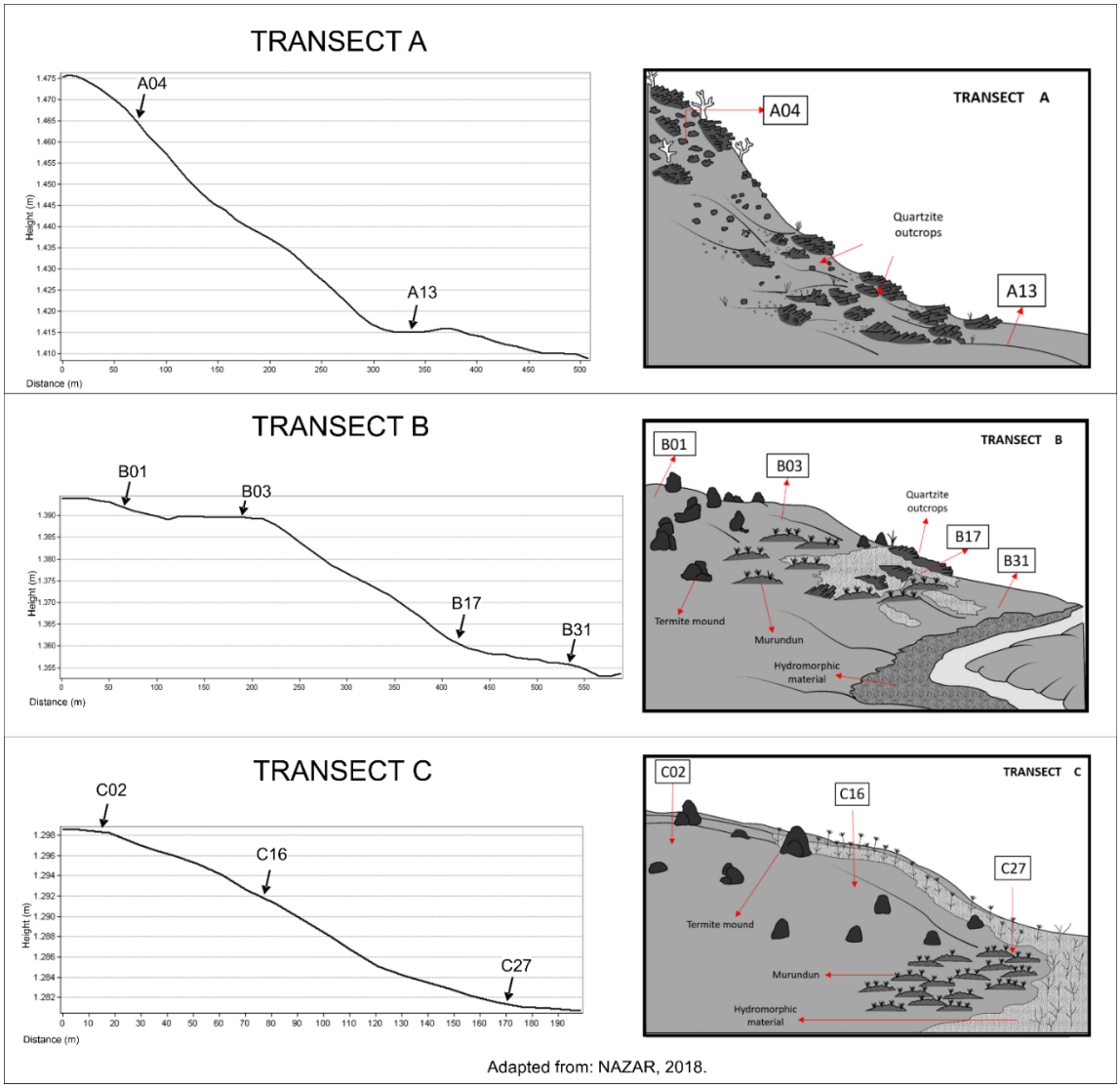

Figure 4. Transects with location of samples and sketch of the landscape situation.

The landscape of the study area shows the occurrence of planation surfaces, embedded valleys with alluvial deposits, and quartzite crests with talus deposits. There are also marks related to the structural control associated with tectonic efforts, such as feature alignments and fracture lines, providing a variety of environments that may contribute to understanding the geomorphological dynamic of similar regions. Furthermore, this area is situated in a national park, the landscape of which dates back to its original characteristics with a rocky package and preserved geocovers and vegetation, enabling more precise geomorphological analyses.

The mineralogical survey of clays in quartzite areas is considered extremely important, as it may contribute to better understanding of the formation environment of different materials, in addition to providing evidence of the degree of weathering related to the area.

A total of nine samples from each of the three transects were selected for performance of the X-ray Diffractometry analysis based on the following criteria: different slope positions (upper, mid, and lower slope), and relevant variation in the clay fraction of the materials (TABLE 1).

Table 1. Samples selected for XRD analysis, indicating the transect and the positions of the samples on the slope.

Transect	SAMPLES			
	Upper slope		Mid-slope	Lower slope
A – Quartzite outcrops with small soil traps between boulders	A04 (Depth >12cm)		-	A13 (Depth 24-29 cm)
B – Thin litosoils and ferricretes. Rare outcrops.	B01 (Depth <18 cm)	B03 (Depth. 26-54 cm)	B17 (Depth 9-17cm)	B31 (Depth 8-48 cm)
C – Flat surface with oxisoils and ferricretes	C02 (Depth 80-100 cm)		C16 (Depth 20-80 cm)	C27 (Depth 20-40 cm)

Source: The authors (2024)

The mineralogical analyses for identification of the minerals present in the clay fraction were based on the performance of X-ray Diffractometry (XRD) at the X-ray laboratory of the Centro de Pesquisa Professor Manoel Teixeira da Costa (Professor Manoel Teixeira da Costa Research Center) (CPMTC), of the Instituto de Geociências (Geosciences Institute) (IGC) of the Universidade Federal de Minas Gerais (Federal University of Minas Gerais) (UFMG). The X-rays were prepared according to the Clay mineral Diffractometry Methodology developed at the Centro de Pesquisa da Petrobras (Petrobras Research Center). Subsequently, these data were statistically analyzed through the multivariate exploratory technique of Principal Components Analysis (PCA), which reduces a set of correlated variables into a smaller set of independent variables, linear combinations of original variations, designated by principal components. The statistical calculations were carried out using the PAST system, version 6.0.

3. Results

The first sampling area is in Transect A, which is in the relief of quartzite crests, with continuous rocky outcrops on the top and a block field with gravelly-sandy materials in the matrix of the top layer on the mid-slopes. Therefore, material accumulates through colluvial deposition, being trapped within the block field covered with a superficial hydromorphic soil. This slope, which is located to the northeast of ChD, covers a distance of 500 meters from top to base, with convex-rectilinear and concave stretches.

Regarding the sampling points used for the XRD for Transect A, two samples were analysed.:

- sample A4 located at a high slope with a depth of 12 cm, is characterized as colluvial material deposited in a concave area,
- the sample A13, between 24 and 29 cm depth, is characterized by a lower concave-rectilinear slope with some rocky outcrops and presence of organic material on a gravelly-sandy layer.

Both samples were collected from sites covered by material in the middle of rocky outcrops, the fine fraction proportion of sample A4 being composed of 7.68% clay, while sample A13 had 13.68%. Thus, for Sample A4 (Figure 5), the clay minerals kaolinite (Al2Si2O5 (OH)4) and illite ((K, H3O) Al2Si3 AlO10 (OH)2) were found, in addition to silica (SiO2) and graphite (C).

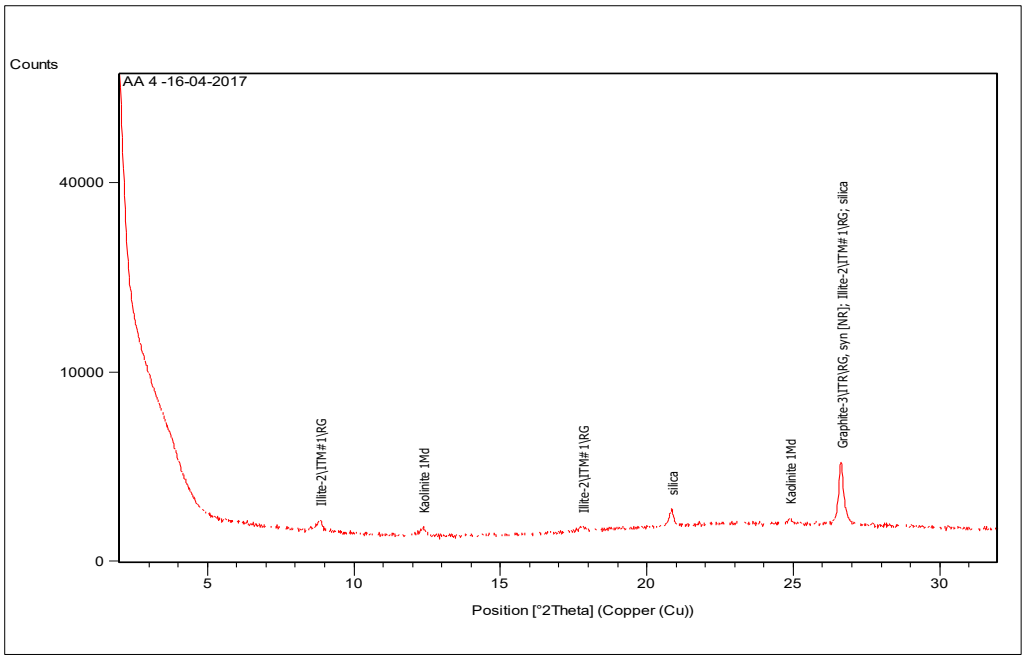

Figure 5. Mineralogy of the clay fraction for Sample A4. The authors (2025)

Regarding Sample A13 (Figure 6), situated on the lower slope, the clay minerals kaolinite and illite were found, with higher peaks than the previous sample, in addition to gibbsite (Al(OH)3).

The results of the principal components analysis (PCA) (Figure 7), together with their eigenvalues (Table 2), based on the contribution of each variable (Table 3), demonstrated the minerals most strongly correlated with Transect A and their respective points, analyzed using XRD.

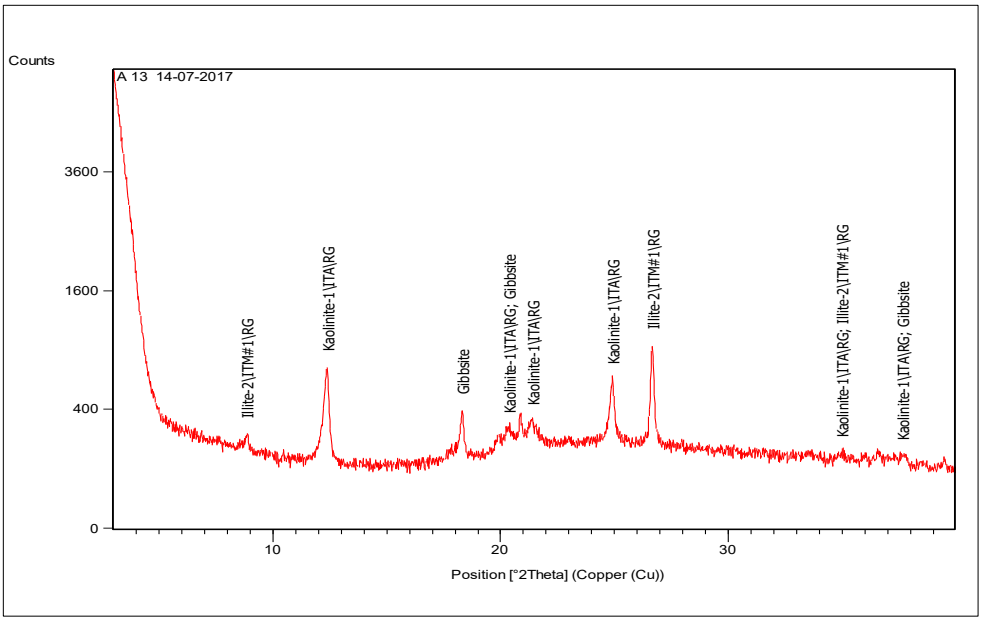

Figure 6. Mineralogy of the clay fraction for Sample A13. Source: The authors (2025)

Thus, kaolinite, gibbsite, and illite are strongly correlated with Sample A13 situated on the lower slope, in a concave-rectilinear segment, whereas silica makes up sample A4, in a concave segment, confirming the quantitative results found through the mineralogy of the clay fraction.

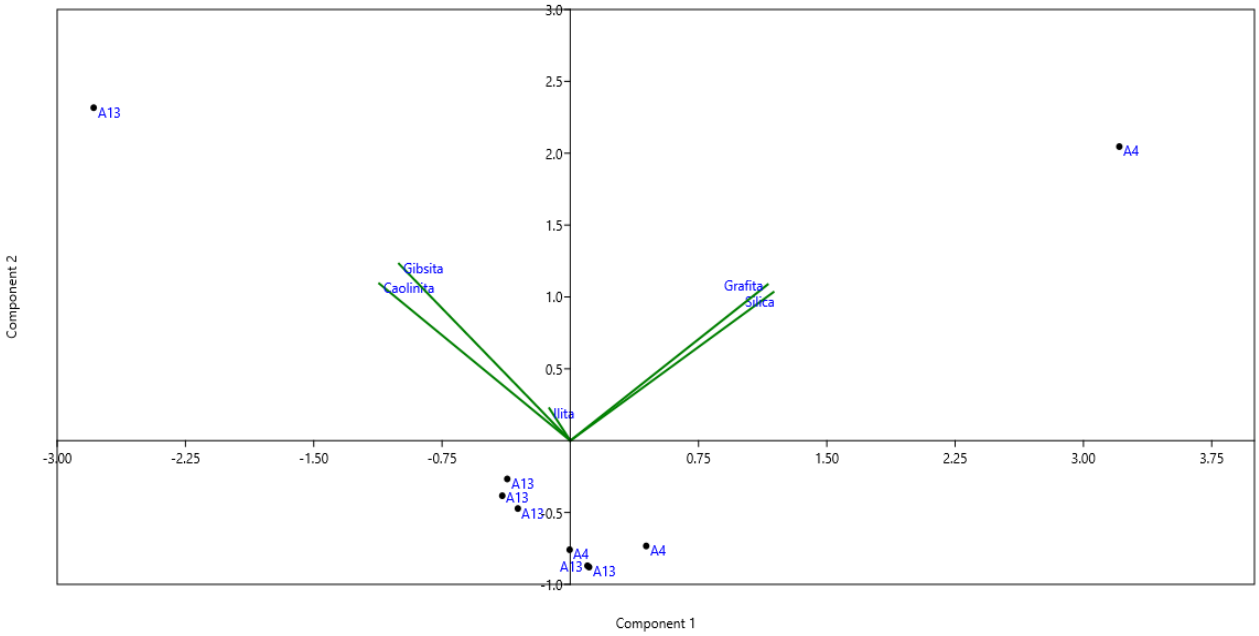

Figure 7. Principal Components Analysis (PCA) based on the diffractogram variables of Transect A.
Source: The authors (2025).

Table 2. Eigenvalues of the factors (principal components) and the statistics correlated with the sampling points of Transect A.

	PC 1	PC 2	PC 3	PC 4	PC 5
A4	3.2098	2.0461	-0.0226	0.0387	-0.0160
A4	-0.0039	-0.7589	-0.2365	-0.0649	-0.0682
A4	0.4436	-0.7327	-0.2634	-0.3808	0.2071
A13	-2.7867	2.317	-0.3323	-0.1507	-0.0028
A13	-0.3686	-0.2661	2.6317	0.0329	-0.0039
A13	-0.3976	-0.3831	-0.4611	0.5151	0.0536
A13	-0.3066	-0.4721	-0.4554	0.3877	0.0261
A13	0.1003	-0.8703	-0.4303	-0.1823	-0.0964
A13	0.1097	-0.8796	-0.4297	-0.1956	-0.0993

Source: The authors (2024)

Table 3. Contribution of each variable of Transect A, based on covariance, for each of the first five principal components (factor).

	PC 1	PC 2	PC 3	PC 4	PC 5
Illite	-0.0546	0.1002	0.9912	-0.0655	0.0007
Kaolinite	-0.4991	0.4883	-0.0308	0.6991	0.1504
Silica	0.5307	0.4617	-0.0243	0.0961	0.7038
Gibbsite	-0.4476	0.5499	-0.1253	-0.6832	-0.1209
Graphite	0.5156	0.4856	0.0085	0.1756	-0.6836

Source: The authors (2024)

The second sampling area with Transect B, which was located on a flat relief smoothly dissected with rare outcrops and narrow layers of gravelly material concreted on the top, passing through a field of mounds (a set of small protuberances of relief, formed through termite activity in areas with seasonally high moisture conditions on soil, on the mid-slope and peaty materials on the valley floor. Along the upper and mid-slope sections, gravel occurrences with ferruginous concretions were observed, along with a hardened layer of laterite, which was difficult to bore. This slope is around 600 meters long, with convex-rectilinear and concave-rectilinear stretches. Figure 4

Regarding Transect B, the samples used for XRD were:

- Sample B01, on the rectilinear upper slope. The samples were collected from the depth of 0-18 cm, characterized by a gravelly-sandy layer with abundant ferruginous concretions, whereby, below 18 cm there is a iron pan that made further boring impossible.
- Sample B03, on the rectilinear upper slope. From 26 to 54 cm deep, is generally characterized by gravelly-sandy material, with ferruginous concretions.
- Sample B17, Samples was collected from 9 to 17 cm deep, on the mid-slope, soon after the declivity rupture, is characterized by material overlaying the altered quartzite. r.
- Sample B31, on the concave-rectilinear lower slope, from 8 to 48 cm deep, is sandy material with little gravel. This segment of the slope is concave-rectilinear.

Sample B01 (Figure 8), with a clay fraction of 9.7%, had iron and aluminum oxides and hydroxides, such as hematite (Fe2O3), goethite (FeO (OH)), and gibbsite (Al(OH)3), as well as nacrite (Al2Si2O5 (OH)4), an clay mineral of the kaolinite group. The presence of hematite reinforces the color of the materials at the site, being formed of gravels with ferruginous concretions and meaning very reddened tones.

Also, on the upper slope of Transect B, Sample B03 (Figure 9), reflects the occurrence of ferruginous concretions, consisting hematite and gibbsite (main oxides forming laterite), in addition to kaolinite and muscovite (KAl2 (Si3Al) O10 (OHF)2.

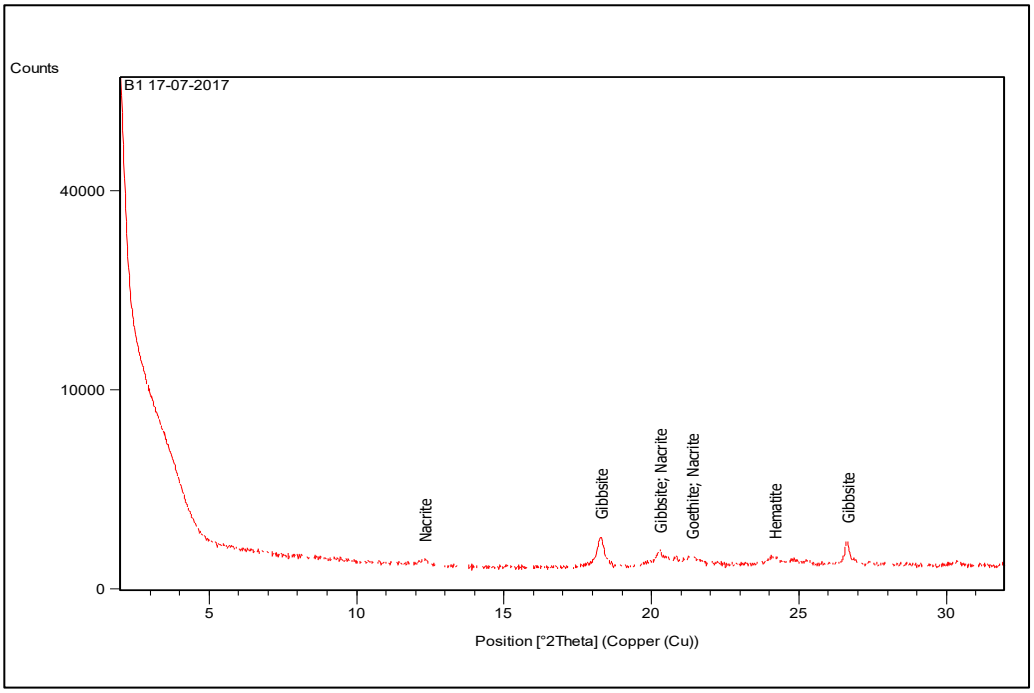

Figure 8. Mineralogy of the clay fraction for Sample B01.Source: The authors (2025)

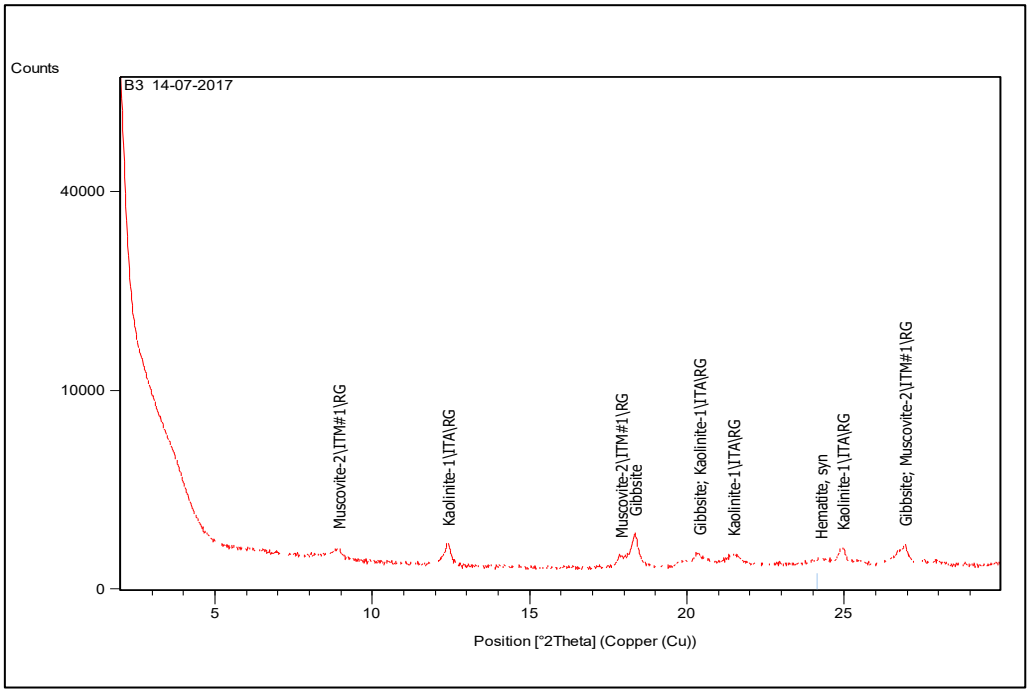

Figure 9. Mineralogy of the clay fraction for Sample B03. Source: The authors (2025)

On the mid-slope of Transect B, Sample B17 (Figure 10) has muscovite ((K, Na) (Al, Mg, Fe)2 (Si3Al0.9) O10 (OH)2), gibbsite, and kaolinite.

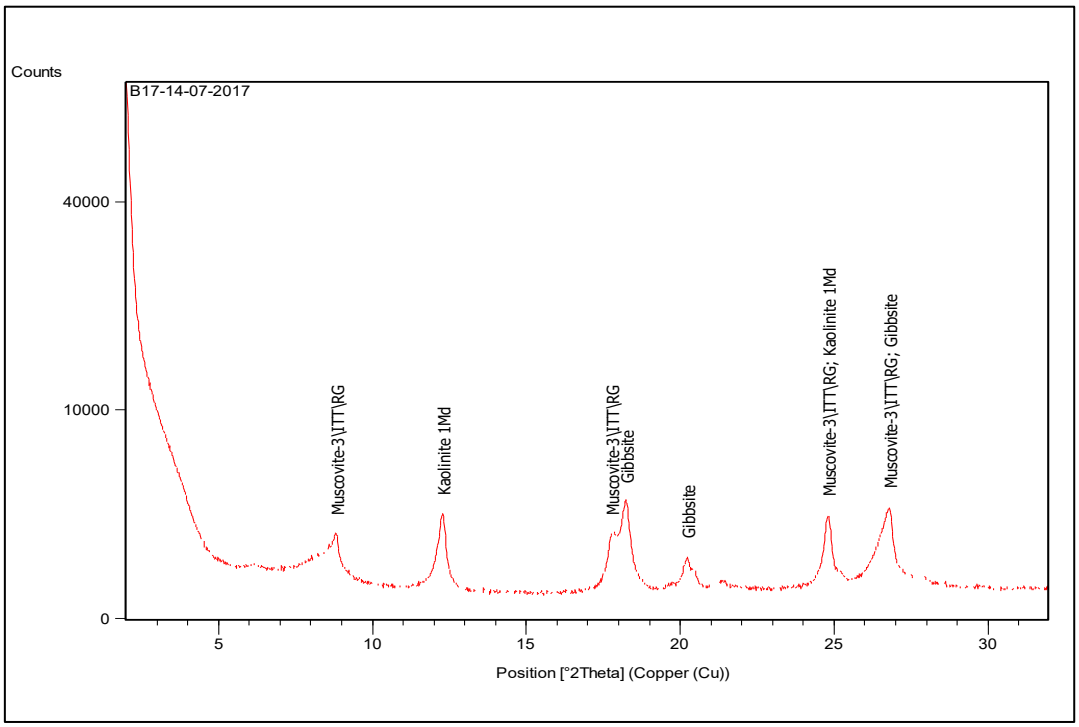

Figure 10. Mineralogy of the clay fraction for Sample B17. Source: The authors

For Sample B31 (Figure 11), gibbsite, kaolinite, and vermiculite ((Mg, Al)3 (Si Al)4 O10 (OH)24 H2O) were identified.

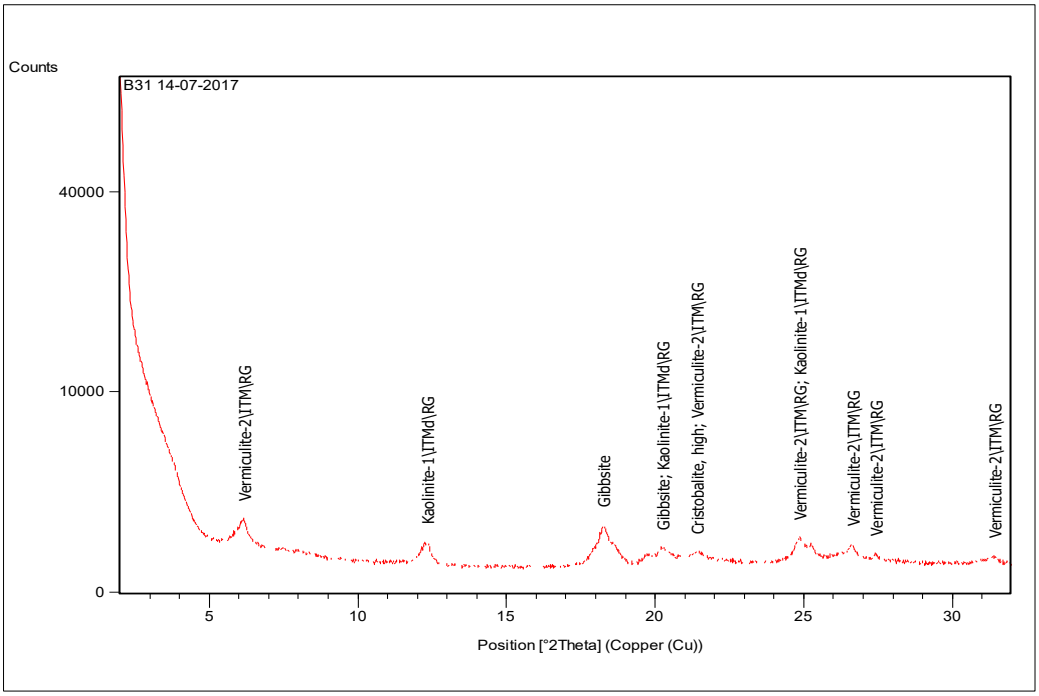

Figure 11. Mineralogy of the clay fraction for Sample B31. Source: The authors (2024)

The mineral with the highest correlation with Sample B1 was nacrite, demonstrated by the 1st quadrant of Figure 12, whereas muscovite, goethite, hematite, and gibbsite are related to Sample B3. For Sample B17 the mineral that most contributed was kaolinite and for Sample B31 it was vermiculite (TABLES 4 and 5).

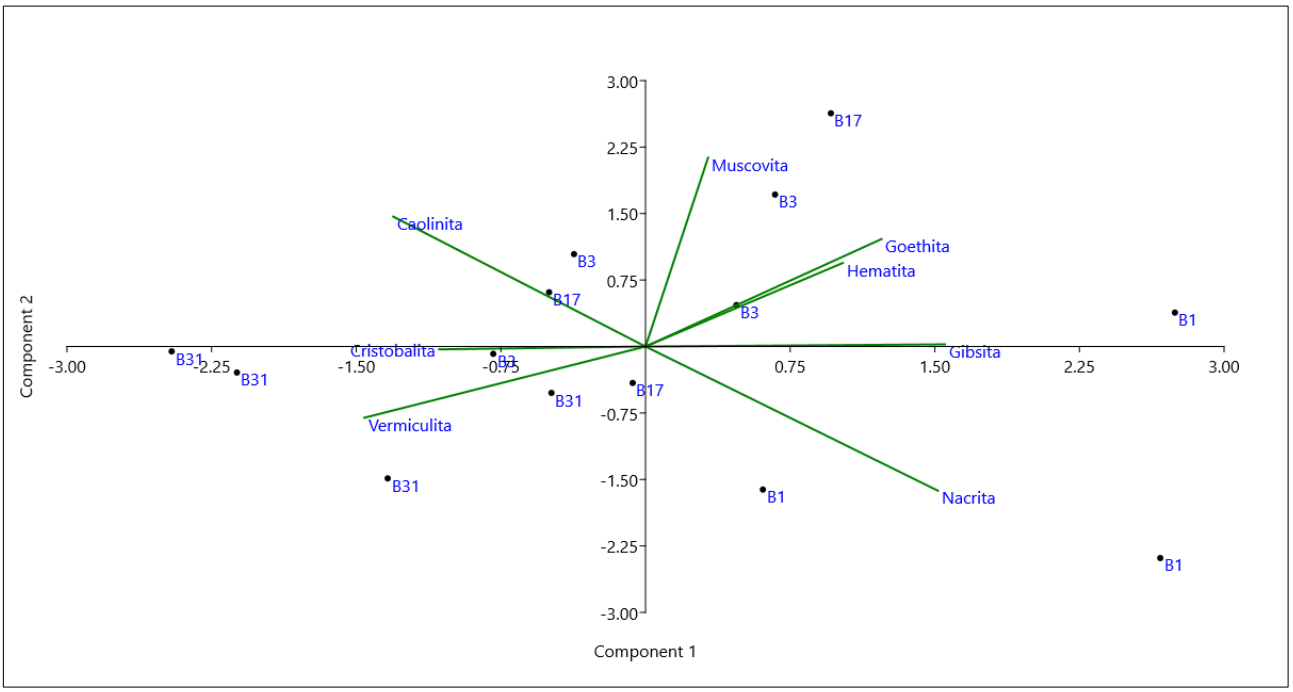

Figure 12. Principal Components Analysis (PCA) based on the diffractogram variables of Transect B. Source: The authors (2024)

Table 4. Eigenvalues of the factors (principal components) and the statistics correlated with the sampling points of Transect B.

	PC 1	PC 2	PC 3	PC 4	PC 5	PC 6	PC 7	PC 8
B1	2.848	0.397	1.032	2.195	0.544	-0.757	-0.162	-0.179
B1	2.769	-2.476	0.980	-1.463	0.073	0.794	-0.105	0.219
B1	0.631	-1.674	-0.802	-0.131	-0.144	-0.755	-0.228	0.594
B3	0.697	1.779	1.0521	0.727	-2.079	0.579	0.394	0.360
B3	0.489	0.485	0.168	-1.110	-0.229	0.755	0.337	-1.000
B3	-0.384	1.081	-1.262	-0.787	-0.065	-0.067	0.391	0.555
B3	-0.819	-0.085	-0.443	-0.070	-0.656	-0.438	-0.899	-0.384
B17	0.997	2.731	-0.353	-0.584	1.795	0.302	-0.262	0.142
B17	-0.518	0.635	-0.989	-0.517	-0.265	-0.217	-0.035	0.210
B17	-0.069	-0.426	-1.291	0.025	-0.113	-0.755	0.538	-0.265
B31	-2.549	-0.056	2.996	-0.790	0.511	-1.012	0.301	0.092
B31	-0.506	-0.543	-0.783	0.184	-0.375	-0.608	-0.228	-0.456
B31	-2.1987	-0.304	0.297	0.826	0.115	1.298	-0.923	0.17
B31	-1.3872	-1.543	-0.600	1.534	0.889	0.882	0.883	-0.010

Table 5. Contribution of each variable of Transect B, based on covariance, for each of the first five principal components (factor).

	PC 1	PC 2	PC 3	PC 4	PC 5	PC 6	PC 7	PC 8
Nacrite	0.43158	-0.46302	0.17231	-0.2295	0.061491	0.08903	-0.2761	0.65502
Gibbsite	0.44218	0.0068435	0.47613	-0.2980	0.034977	0.44881	0.19809	-0.49697
Goethite	0.34835	0.34516	0.11995	0.37208	0.66549	-0.20247	-0.3444	-0.066697
Hematite	0.29121	0.26844	0.32209	0.5768	-0.52856	-0.017268	0.23629	0.26682
Kaolinite	-0.37227	0.4171	0.36082	-0.1881	-0.21901	0.25773	-0.6306	0.099001
Muscovite	0.092361	0.60667	-0.2600	-0.3556	0.19802	0.22484	0.3944	0.42893
Vermiculite	-0.41503	-0.22863	0.16793	0.41703	0.37837	0.59479	0.20608	0.18428
Cristobalite	-0.30448	-0.00902	0.632	-0.2271	0.20591	-0.52782	0.33846	0.14347

The third sampling area is characterized by Transect C, on flat to smoothly dissected relief, with deep materials of clayey-sandy granulometry, and an absence of rocky outcrops. Mounds appear on the lower slope and the organic materials on the valley floor. In general, the soils are uniform with rare occurrences of quartz grains wrapped in iron. This slope is 200 meters long and is convex-rectilinear on its upper part and concave-rectilinear on the lower part.

The following samples were collected along in Transect C:

- Sample C02, on the upper convex slope, at 20 to 100 cm deep, characterized by reddish, fine and deep material, with higher moisture content.
- Sample C16, on the concave mid-slope, 20 to 80 cm deep, brown coloration. From 20 cm, slightly concreted grains appear.
- Sample C27, on the lower concave slope, 20 to 40 cm deep, has multicolor material, a brown layer, with the presence of some gravels with ferruginous concretions.

Figure 13 shows the mineralogy of the clay fraction in Sample C02, in which kaolinite, gibbsite, goethite, and siderite (Fe C O3) have been identified. The latter is an Fe carbonate from the calcite group, which occurs in association with oxides, hydroxides, and silicates.

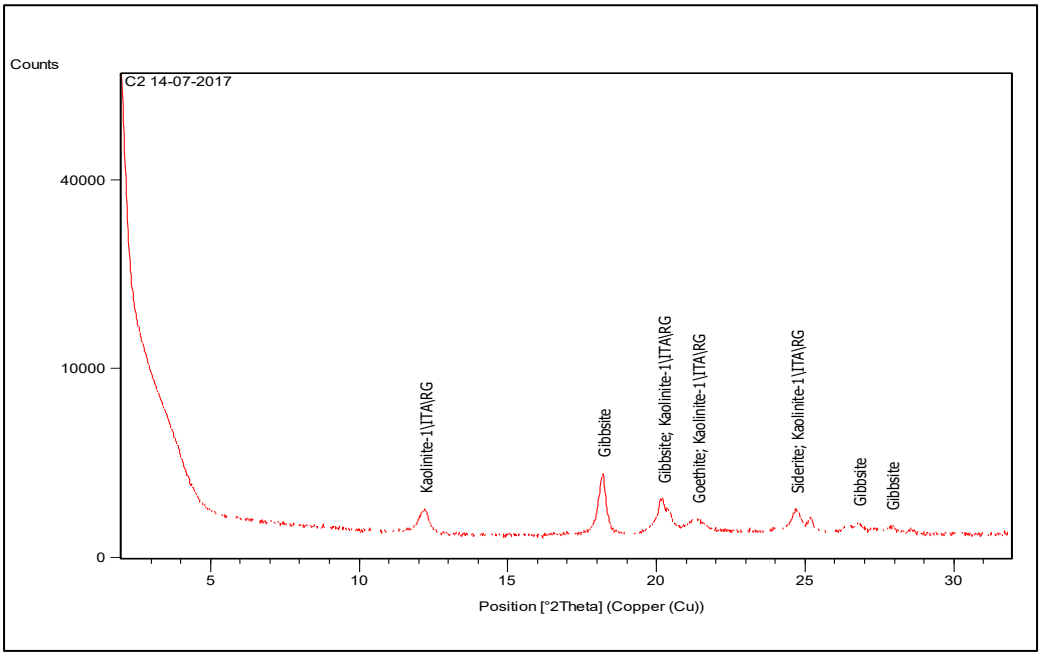

Figure 13. Mineralogy of the clay fraction for Sample C02. Source : The authors

Sample C16 (Figure 14) is characterized by the presence of gibbsite, siderite, clinochlore ferroan ((Mg Al)6 (Si Al)4 O10 (OH)8), and cristobalite (SiO2).

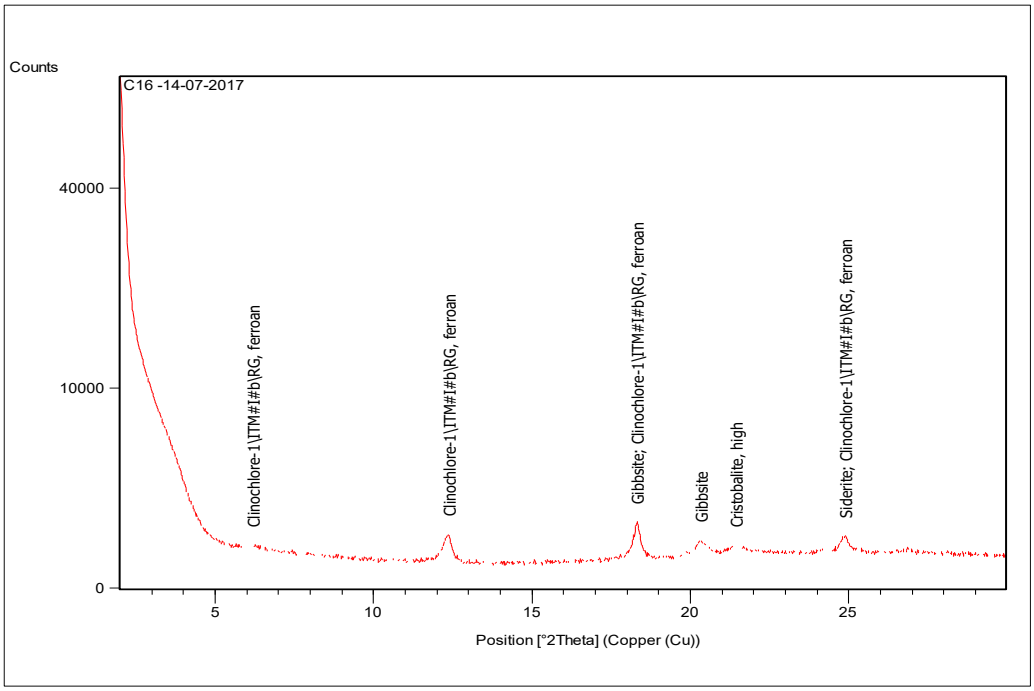

Figure 14. Mineralogy of the clay fraction for Sample C16

Finally, Sample C27 (Figure 15) brings kaolinite, goethite, and gibbsite (final products of weathering), in addition to siderite and biotite (2 (Mg , Fe) O ! (K , H)2 O (Al , Fe)2 O3 ! Si O2), which occur associated with metamorphic rocks in general.

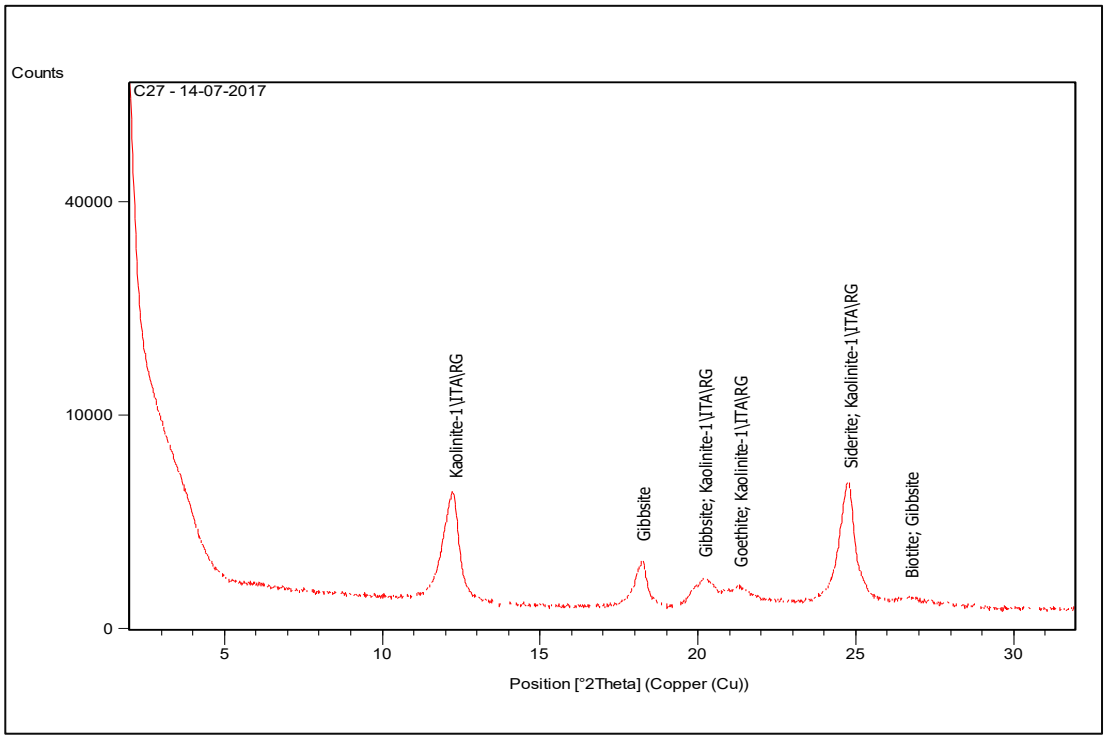

Figure 15. Mineralogy of the clay fraction for Sample C27. Source: The authors (2024)

In Transect C, gibbsite corresponds to point C2 located on the top of the slope; siderite, cristobalite, and clinochlore ferroan correlate with Sample C16 located on the mid-slope; and kaolinite, biotite, and goethite correlate with Sample C27 on the valley floor (Figure 16) (TABLES 6 and 7).

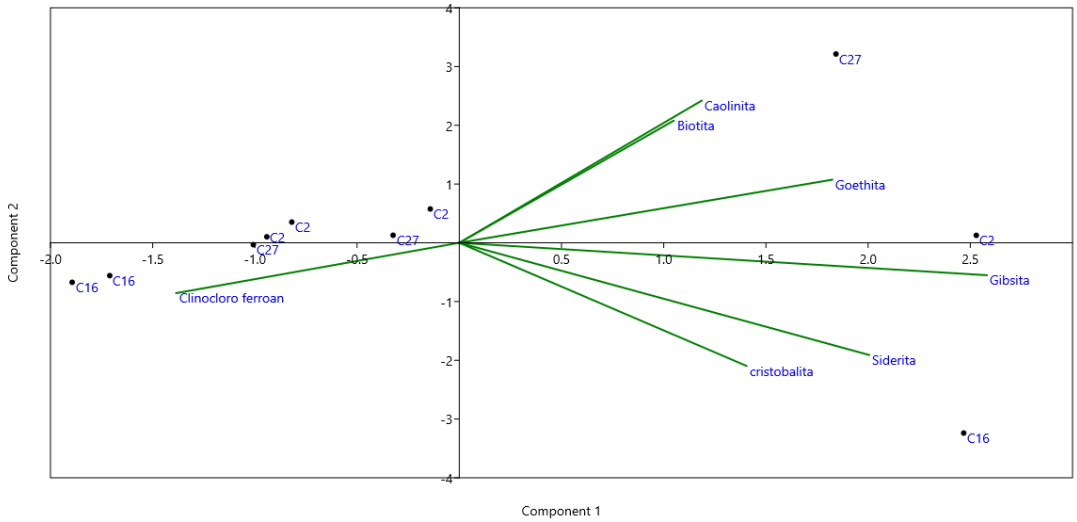

Figure 16. Principal Components Analysis (PCA) based on the diffractogram variables of Transect C. Source: The authors (2024)

Table 6. Eigenvalues of the factors (principal components) and the statistics correlated with the sampling points of Transect C.

	PC 1	PC 2	PC 3	PC 4	PC 5	PC 6	PC 7
C2	2.529	0.126	-2.063	0.534	0.019	0.072	-0.010
C2	-0.142	0.575	0.123	-0.728	0.814	-0.087	-0.029
C2	-0.941	0.103	-0.039	-0.815	-0.219	0.076	-0.021
C2	-0.819	0.352	0.085	-0.826	0.072	0.254	0.066
C16	2.467	-3.238	1.161	-0.108	-0.031	-0.003	0.003
C16	-1.894	-0.672	0.086	1.589	0.113	0.014	0.012
C16	-1.71	-0.558	0.028	1.053	-0.031	-0.014	-0.016
C27	1.842	3.213	1.264	0.645	-0.156	-0.008	-0.001
C27	-0.323	0.128	-0.540	-0.533	-0.203	-0.285	0.065
C27	-1.007	-0.031	-0.106	-0.809	-0.376	-0.018	-0.068

Table 7. Contribution of each variable of Transect C, based on covariance, for each of the first five principal components (factor).

	PC 1	PC 2	PC 3	PC 4	PC 5	PC 6	PC 7
Kaolinite	0.262	0.535	0.267	-0.024	0.625	0.380	0.188
Gibbsite	0.571	-0.122	-0.142	0.126	0.392	-0.642	-0.236
Goethite	0.403	0.237	-0.615	0.311	-0.321	0.161	0.417
Siderite	0.443	-0.422	0.033	0.069	-0.066	0.617	-0.481
Clinochlore ferroan	-0.306	-0.189	0.096	0.893	0.240	0.047	0.047
Cristobalite	0.311	-0.463	0.487	-0.047	-0.105	-0.059	0.658
Biotite	0.232	0.460	0.530	0.284	-0.526	-0.169	-0.256

4. Discussion

Our analyses made it possible to associate mineralogical aspects of the geocovers with topographic positions in slope segment, enabling the inference of relationships between the processes that occur in response to a given climate type according to lithological characteristics and relief. Studies carried out by Santos e Confessor (2020) and Rodrigues et al (2023b) using Optically Stimulated Luminescence Single Aliquote Regeneration (OSL/SAR) and radiocarbon dating in the same study area demonstrated that the slope deposits, in more than 10 different locations, are all very recent, mostly more recent than the Middle Holocene.

The results allowed better understanding of the degrees of weathering of the Chapadão do Diamante (ChD) group, as an area representative of quartzite relief. In general terms, these regions are recognized for the resistance of the materials to weathering agents, whereby high-level weathering action results in the occurrence of silicated clays (clay minerals), and extremely resistant products such as iron and aluminum oxides and hydroxides. In addition to the identification of the results of advanced weathering on certain slope segments, the analyzed materials also enable identification of some constituent minerals of the rocks that are present.

In their studies on tropical regions, Pereira et al. (2020) found more higher rate of weathering and resulting in chemical alteration and deeper weathering mantles developed superficial materials than in cold environments, due to the high temperatures and rains, which mainly facilitate the hydrolysis of silicates. The profiles analyzed by the authors was deep and present changes related to the neoformation of clay minerals that are synthesized from ionic or colloidal products originating from weathering. Kaolinite is the dominant clay mineral (Pereira et al., 2020), and, in many situations, is associated with large concentrations of Fe and Al oxides, in addition to the presence of illite and montmorillonite in some cases.

The differences observed both in the field and based on the physical and mineralogical analyses, may be associated with the complex landscape of ChD, the coverage of which may serve for analyses of quartzite regions in general. Thus, the litho-structural aspects, the forming of the relief, and the different types of geocovers, whose interdependence can be verified based on the spatial analyses carried out by Nazar and Rodrigues (2020), present representative responses, considering the prolonged action of a humid tropical climate. These responses are shown in the granulometric analysis, previously presented by Nazar and Rodrigues (2019a), and in x-ray diffractometry, presented in this study.

The mineralogy of the clay fraction of the samples from Transect A reflects the game of forces between the resistance of the parent material and the intensity of weathering in a tropical environment, associated with the topographic question when analyzing the concave and concave-rectilinear segments from which the samples were taken. We understand that the landscape group, in its various combinations, may distinguish materials with different responses and behaviors. Therefore, the results of the analyses may be associated and interpreted together with other surveyed data on the area and the geomorphological environment in which it is located.

Regarding Sample A4 which is located in a high concave slope segment insert as a trap in the middle of quartzite blocks, it is associated with the presence of the clay mineral illite, which corresponds to a type of hydrated mica, and to the moisture content in the environment (subsurface drainage), with the availability of aluminum and potassium cations. The kaolinite, in turn, is indicative of highly weathered bedrock, which suggests that the sampling point has been in a stable environment for a long time, under the action of a humid tropical climate.

However, in general, we understand that despite the sample inserted in an environment of quartzite crests, whose characteristics were described as predominantly gravelly-sandy, with geocovers of little thickness and a low degree of alteration as a result of their greater resistance to weathering processes, the presence of 1:1 clay minerals reflects the intense and prolonged action of water in this environment. In other words, small structural traps, as concaves segments between blocks, enable the storage of quartzite weathering products and their geochemical evolution, being found at a topographic position in a framework on the upper slope, which enables alternate exposure to dry and humid epochs.

Sample A13, which is found on the lower concave-rectilinear slope with some rocky outcrops, indicates a more elevated state of weathering when compared to Sample A4. Gibbsite results from the loss of silica from the clay minerals, being one of the most common aluminum oxides found on the Earth's surface. The highlighted illite peaks indicate longer permanence of water at the site, facilitated by the concave-rectilinear topography in a structural terrace situation controlled by bedrock, where the flow dynamic suffers a deceleration as a result of the loss of potential energy associated with the low declivity of the land.

The correlation of the variables and the graph representing PCA (Figure 4) enabled characterization of the minerals that most stood out in the formation and differentiation of the environments. Thus, a considerable presence of illite, kaolinite, and gibbsite can be observed in Sample A13. These results were useful for the landscape interpretation and corroborated the general observations in the study by Rossetti et al. (2005), which presents the illitization process that can occur with or without the presence of smectite and can form from a precursor mineral such as kaolinite, provided there is an adequate supply of K (potassium) in the area, the presence of which in ChD has been identified in studies by Nazar (2018) and Santos (2021).

Silica is observed as another mineral strongly related to point A4 and due to its location in a slope surrounded by quartzite blocks which are the source of the deposit, where there is a predominance of developed immature materials, certainly related to the lithology of the region. Studies in quartzite regions by Rezende et al. (2010), state that chemical denudation rates are not clearly conditioned by the landscape position but appear to be controlled by the geology.

Transect B which is located in flat surface on the upper part and develops a convex-rectilinear and concave-rectilinear stretches, presented the occurrence of Fe and Al oxides and hydroxides, demonstrating the advanced degree of weathering in the area, and which may constitute lateritic geocovers when in large quantities. Hematite is indicative of a well-drained environment, although the presence of goethite reflects a transition, given that it occurs in environments with deficient drainage. This situation illustrates the presence of water in the surface materials at different topographic levels throughout the ChD, the dynamic of which is extremely interesting for future research.

In a study on mineralogy of tropical surface materials, Pereira et al (2020) analyzed the hematites formed from ferrihydrite, which is a less crystalline phase of aggregation, dehydration, and structural rearrangement, provided conditions are favorable with low silica activity in solution and small quantities of organic material, the results of which are low complexation of Fe (KÄMPF AND CURI, 2000; SCHAEFER, 2008 apud PEREIRA et al., 2020). According to the same author, these conditions are specific to systems with free drainage and high temperatures, with enough water to cause high alteration rates and silica leaching, which could justify the strong correlation of minerals demonstrated in Figure 9. By associating these conditions with the topography of the area of occurrence of the samples from Transect B, which is smoother and with flat peaks, it is possible to infer that the geomorphological evolution occurred more intensely than in Transect B.

Regarding the presence of muscovite in Sample B03 from the upper slope with low declivity and close to the interfluve, it is believed to be a primary mica resulting from the composition of micaceous quartzites. As it is a phyllosilicate of difficult weathering decomposition, remaining for longer in the environment, this may be associated with the dominant presence of rocky outcrops, isolated blocks, and low thickness of the weathering mantle.

The chemical composition of muscovite, containing basically constituted of aluminum, sodium, or potassium, may often present iron and crystalized magnesium, among other elements (SIMÕES, 1995). In Sample B17, the muscovite appears with the following composition: (K , Na) (Al, Mg, Fe)2 (Si3.1 Al0.9) O10 (OH)2, Fe being one of the constituents. This evidence may be explicative of the origin of Fe in the central and western areas of the ChD, being constituted of micaceous quartzites interspersed with muscovite phyllites, as described by Simões et al. (2015).

On the lower concave -rectilinear slope, in Sample B31, in a situation of hydromorphism, vermiculite stands out. This is a 2:1 clay mineral with an intermediate degree of weathering, formed through hydration, which can generally be associated with biotite and chlorite decomposition. Its occurrence on the lower slope segment may indicate a poorly drained environment associated with the proximity of the main channel of the basin, the São Francisco River.

In relation to weathering of micaceous minerals and transformation into 2:1 mineral, evidence from laboratory tests and field observations has shown the greater capacity of vermiculite to be altered as a result of climate warming and wetting, which is comparable to muscovite (ROSSETTI et al., 2005; SPARKS, 1987).

Transect B has a strong presence of the element potassium (K). As such, the potassium is released from feldspars by the action of water and weak acids through hydrolysis and/or protonation reactions (Santos, 2021; Fanquim, 2005). When there is total hydrolysis, the weathering of the feldspar results in the release of potassium to the solution and in the production of gibbsite, even when concerning sites with low weathering rates such as the Ridge areas of quartzite mountain massifs where the sample was collected.

In Transect C, Sample C02 on the upper convex slope goethite was found, indicating a poorly drained environment, with water remaining in the system for longer, the same being valid for siderite, which, according to Postma (1980), can be formed from the reduction of iron oxides/hydroxides and the dissolution of calcium carbonate (CaCO3). Furthermore, in the view of Retallack (1990), inert subterranean water enables the persistence of chemically reduced minerals, such as siderite. This premise is consistent with the presence of subsurface moisture noted along the bore holes in Transect C.

Clinochlore is a clay mineral from the chlorites group, being, in this case, associated with Fe2+. It is common on metamorphic rocks, in addition to possibly being the result of biotite alteration (KLEIN, DUTROW, 2012). The cristobalite, however, is a polymorphous variation of quartz (MACHADO et al., 2017). These conditions indicate a high degree of weathering through the presence of aluminum oxide, as it is one of the last, most resistant, residual products of mineral weathering. The presence of siderite indicates a poorly drained environment, and together with the clinochlore ferroan, confirms the influence of iron at that location.

In summary, it can be stated that the constituents of the clay fraction at the sampling points along Transect C, which is the transect located far from the outcrops of quartzite indicate a high degree of weathering, due to the occurrence of 1:1 clay minerals and aluminum and iron oxides and hydroxides. The presence of hydrated minerals, such as siderite and goethite, is the response to insufficient drainage of the area, and the occurrence of clay minerals from the chlorites group may indicate a change in the rocky substrate, since the slope in question is located in the vicinity of the rocks of the Paracatu Indivisa Formation of the Canastra Group, in the western sector of Chapadão do Diamante, with muscovite-chlorite-quartz schists, in a flat surface.

However, other investigations suggest that the formation of gibbsite from aluminum silicates passes through intermediate clayey minerals, including the progressive dissolution of kaolinite (desilification) (MILLOT, 1964). This is reported because the proportion of kaolinite and gibbsite is generally inversely related, whereby gibbsite represents the dominant mineral in highly altered surface materials and kaolinite is the dominant mineral in less weathered zones, as indicated in the studies of Santos (2021) and Nazar (2018).

5. Conclusions

Considering the morphological diversity of the recognized geocovers for the quartzite peaks of the Serra da Canastra (Chapadão do Diamante - ChD), three sampling areas were selected on different patterns observed as being representative of the landscape, to contribute to a deeper understanding of the landscape. The application of the X-ray Diffractometry (XRD) laboratorial analyses contributed to the mineralogical characterization of the materials, and the multivariate exploratory technique of Principal Components Analysis (PCA) enabled the establishment of correlations between the multiple minerals analyzed. This enabled better understanding of the associations between the minerals, in addition to leading to understanding of the degrees of weathering in the three environments.

This study showed that mineralogical analyses of geocovers in quartzite areas in a humid tropical environment may indicate that these areas represent of the equilibrium between the resistance of the quartzite parent material and the weathering intensity when the topography is one of the factors in the analysis. In other words, we showed that the three observed transects present significant differences in relation to rocky substrate, whereby Transects A and B enabled the recognition of quartzite, be it pure or micaceous, enabling the inference that the topography is an important factor for the development of weathering mantles. Transect C, however, enabled the inference of a change in the lithology, because quartzites outcrops are not visible on the landscape.

The topographic variation, due to the alternation of concave segments of the slopes and the presence of natural barriers, can be understood as a relevant factor for the formation of clay minerals such as kaolinite and gibbsite, which denote areas that were under strong weathering action. On the other hand, the flat divides, which have the presence of Fe oxides and hydroxides, also indicate advanced weathering of the rocks, even in geocovers of little thickness. This may indicate that the environment has been stable for a long time. It can be noted that in incipient materials formed through processes of transport through gravity (colluvial materials), the pedogenetic activity is present in competition with the resistance of the quartzite rocks.

The same is valid for the areas with residual ferruginous materials, where the presence of muscovite was found with iron in its chemical composition, this being mica, one of the components of the micaceous rocks and micaceous quartzite present there. It is estimated that the long exposure to weathering led to the complete

degradation of this muscovite in the areas where the geocovers of ferruginous materials prevail. Such a hypothesis is adjusted to the theory that the deeper, reddish, ferruginous materials of Brazil under a seasonal tropical climate originate from in-situ formation (autochtone).

Authors contributions: Concept, S.C.R.; Methodology, S.C.R, T.I.S.M.N and F.C.S.; Software, T.I.S.M.N and F.C.S.; Validation, T.I.S.M.N, L.P and F.C.S.; Formal Analysis, S.C.R, T.I.S.M.N, L.P and F.C.S.; Research, S.C.R, T.I.S.M.N and F.C.S.; Resources, S.C.R.; Data preparation, T.I.S.M.N and F.C.S.; Manuscript writing, S.C.R, T.I.S.M.N, L.P and F.C.S.; Revision, S.C.R, T.I.S.M.N and L.P.; Supervision, S.C.R.; Financing acquisition, S.C.R. All authors read and agreed to the final version of the manuscript.

Funding: This research was funded by CNPq, through resources granted by Chamada Universal (Process: 403412/2023-4); Bolsa PQ/CNPQ (Process 302924/2019-1) and PRINT/CAPES/UFU 88887.311505/2018-00

Acknowledgments: We would like to thank the reviewers of this article for their contributions

Conflict of interest: The authors declare that there is no conflict of interest.

References

1. CAMPY, M.; MACAIRE, J.J. Géologie des formations superficielles: géodynamique – faciès - utilisation. Paris; Milan, 1989. 433 p.
2. EMBRAPA. Sistema Brasileiro de Classificação de Solos. Brasília, DF: Embrapa, 2018. 355p.
3. FANQUIM, V. Nutrição Mineral de Plantas. Curso de PósGraduação "Lato Sensu" (Especialização): Solos e Meio Ambiente. Lavras: UFLA/FAEPE, 2005. 182 p.
4. KLEIN, C. DUTROW, B. Manual de ciência dos minerais. Tradução e revisão técnica: Rualdo Menegat. 23 ed. Porto Alegre: Bookman, 2012.
5. MACHADO, F.B.; MOREIRA, C.A.; ZANARDO, A; ANDRE, A.C.;GODOY, A.M.; FERREIRA, J. A.; GALEMBECK, T.; NARDY, A.J.R.; ARTUR, A.C.; OLIVEIRA, M.A.F. Enciclopédia Multimídia de Minerais. [on-line]. ISBN: 85-89082-11-3 Disponível em <http://www.rc.unesp.br/museudpm>. Acesso em novembro de 2017.
6. MILLOT, G. Géologie des argiles: altérations, sédimentologie. Paris : Masson & Cie, 1964. 425p.
7. NAZAR, T. I. S. M. O Chapadão do Diamante na Serra da Canastra/MG, Brasil: caracterização geomorfológica e análise integrada do meio físico a partir de dados multifontes. Tese (Doutorado em Geografia) – Universidade Federal de Uberlândia, Uberlândia, 2018. 270 f. http://dx.doi.org/10.14393/ufu.te.2018.608
8. NAZAR, T. I. S. M.; RODRIGUES, S. C. Mapeamento e Análise de Geocoberturas no Chapadão do Diamante – MG – Brasil. Mercator, Fortaleza, v. 18, p. 1-19, 2019a. DOI: 10.4215/rm2019.e18010.
9. NAZAR, T. I. S. M.; RODRIGUES, S. C. Relevo do Chapadão do Diamante, Serra da Canastra/MG, Brasil: compartimentação e análise a partir dos aspectos geomorfométricos. Revista Brasileira de Geomorfologia, v. 20, p. 69-88, 2019b. DOI: 10.20502/rbg.v20i1.1300
10. NAZAR, T.I.S.M.; RODRIGUES, S.C. Análise comparativa de geocoberturas em três vertentes no Chapadão do Diamante, Serra da Canastra-MG, Brasil. Caderno de Geografia, v.30, Número Especial 1, 2020. DOI: 10.5752/P.2318-2962.2020v30nesp1p1-18
11. NOVAIS, G. T. Caracterização climática da mesorregião do Triângulo Mineiro/Alto Paranaíba e do entorno da Serra da Canastra (MG). 2011. 189 f. Dissertação (Mestrado em Ciências Humanas) - Universidade Federal de Uberlândia, Uberlândia, 2011. https://repositorio.ufu.br/handle/123456789/16101
12. PEREIRA, T.T.C.; OLIVEIRA, F.S.; FREITAS, D.F.; DAMASCENO, B.D.; DIAS, A.D. A Mineralogia dos Solos Tropicais: Estado da Arte e Relação com o Uso e Manejo. Geonomos, v.28 n.1, p. 1-14, 2020. DOI: 10.18285/geonomos.v28i1.29650
13. POSTMA, D. Formation of siderite and vivianite and the pore-water composition of a Recent bog sediment in Denmark. Chemical Geology, v. 31, p. 225-244, 1980. DOI: 10.1016/0009-2541(80)90088-1
14. QUEIROZ NETO, J. P. O estudo de formações superficiais no Brasil. Revista do Instituto Geológico. São Paulo, v. 22, n. 1/2, p. 65-78, 2001. DOI: 10.5935/0100-929X.20010003
15. REZENDE É. A, LEÃO M. R., SALGADO A. A. R, OLIVEIRA C. K R DE, JÚNIOR H. A. N. A influência litológica nas taxas de denudação geoquímica do médio Espinhaço Meridional – MG. Sociedade & Natureza, Uberlândia, v.22, n.3, p. 503-514, dez. 2010. DOI: 10.1590/S1982-45132010000300007
16. RETALLACK, G.J. Soils of the past: An introduction to paleopedology. London: Unwin Hyman. 1990. DOI: 10.1007/978-94-011-7902-7
17. RODRIGUES, S.C,, DOS SANTOS, F.C, CARVALHO, R.F.F, NAZAR, T.I.S.M. Chronology Of Quartzitic

Slopes From Minas Gerais, Brazil. *Mercator, 21*. (2023b). DOI: 10.4215/rm2022.e21032.

18. RODRIGUES, S. C., AUGUSTIN, C. H .R. R., NAZAR, T. I. S. M. Mapeamento Geomorfológico do Estado de Minas Gerais: uma proposta com base na morfologia. Revista Brasileira de Geomorfologia, v.24, n.1. 31p. (2023a). DOI: 10.20502/rbg.v24i1.2233
19. ROSSETTI, D. F.; TOLEDO, P. M.; GÓES, A. M. New geological framework for Western Amazonia (Brazil) and implications for biogeography and evolution. Quaternary Research, v. 63, p.78-89, 2005. DOI: 10.1016/j.yqres.2004.10.001
20. SANTOS, F.C. As formações superficiais do Chapadão do Diamante - Serra da Canastra: Contributo Geoquímicos, Físicos e Geocronológicos. Tese (Doutorado em Geografia) - Universidade Federal de Uberlândia, Uberlândia, 2021. 177 f. DOI: 10.14393/ufu.te.2021.5526
21. SANTOS, F.C., CONFESSOR, J.G., Geoquímica e geocronologia em campos de murunduns no Chapadão do Diamante –Serra da Canastra-MG. Caderno de Geografia, 30, n.esp. 1, 99-111. 2020. DOI: 10.5752/P.2318-2962.2020v30nesp1p99-111
22. SIMÕES, L.S.A. Evolução tectono-metamórfica da Nappe de Passos, sudoeste de Minas Gerais. Tese (Doutorado em Geociências). Instituto de Geociências, USP, São Paulo, 1995. 149 f.
23. SIMÕES, L.S.A.; MARTINS, J.E.S.; VALERIANO, C.M.; GODOY, A. M.; ARTUR, A. C. Folha Vargem Bonita, SF.23-V-B-I. Projeto Fronteiras de Minas Gerais. Programa Mapeamento Geológico do Estado de Minas Gerais. Contrato CODEMIG 3473, FUNDEP 19967. UFMG: 2015.
24. VALERIANO, C. M.; DARDENE, M. A.; FONSECA, M. A.; SIMÕES, L. S. A.; SEER, H. J. A evolução tectônica da Faixa Brasília. In: MANTESSO-NETO, V. et al. (Org.). Geologia do continente sul-americano: evolução da obra de Fernando Flávio Marques de Almeida. São Paulo: Beca, 2004. p. 575-592
25. VIDAL-TORRADO, P; LEPSCH, I. F.; CASTRO, S. S.; COOPER, M. Pedogênese em uma sequência latossolo-podzólico na borda de um platô na depressão periférica paulista. R. Bras. Ci. Solo, V.23, n.4, p.909-921, 1999. DOI: 10.1590/S0100-06831999000400018